IEEE Access
Multidisciplinary ⋮ Rapid Review ⋮ Open Access Journal

Received March 3, 2021, accepted March 23, 2021, date of publication March 26, 2021, date of current version April 5, 2021.

Digital Object Identifier 10.1109/ACCESS.2021.3069103

On the Bit Error Probability and the Spectral Efficiency of Opportunistic Wireless Transmissions in Rician Fading Channels

NATHALY OROZCO GARZÓN[1], HENRY CARVAJAL MORA[1], (Member, IEEE), FERNANDO ALMEIDA GARCÍA[2], AND CARLOS DANIEL ALTAMIRANO[2,3], (Member, IEEE)

[1]Faculty of Engineering and Applied Sciences (FICA), Telecommunications Engineering, Universidad de Las Américas (UDLA), Quito 170125, Ecuador
[2]School of Electrical and Computer Engineering, University of Campinas (UNICAMP), Campinas 13083-852, Brazil
[3]Department of Electrical and Electronics (DEEL), Universidad de las Fuerzas Armadas-ESPE, Sangolqui 171103, Ecuador

Corresponding author: Henry Carvajal Mora (henry.carvajal@udla.edu.ec)

This work was supported by the Universidad de Las Américas (UDLA), Quito, Ecuador under Project ERT.HCM.20.01.

ABSTRACT Opportunistic systems take advantage of the wireless communication channel random behavior, since transmission is made only when fading amplitude is above a threshold value, which is calculated based on a transmission probability. This type of transmission draws attention because improves the system performance, and it is an interesting scheme for primary users in cognitive radio networks or is also an option for physical layer security. In this paper, we analyze the performance of opportunistic transmissions in Rician fading channels considering square-quadrature-amplitude-modulation (S-QAM) and non-square-quadrature-amplitude-modulation (NS-QAM). Exact closed-form expressions and approximations are derived to evaluate the average bit error probability (ABEP). An expression to calculate the mean spectral efficiency (SE) is also derived considering that a target ABEP must be guaranteed. The SE is calculated using the coverage radius obtained for each modulation used in the system. Hence, an algorithm for the radii calculation is also presented, which considers that the parameters of the Rician fading channel change in the cellular area. The results show that opportunistic transmission (OpT) mitigates the fading effects once the ABEP decays exponentially as the signal to noise ratio (SNR) is increased. Additionally, the proposed algorithm, along with the derived expressions, determine the scenarios where the SE is maximized.

INDEX TERMS Opportunistic system, Rician fading channel, modulations, bit error probability, spectral efficiency.

I. INTRODUCTION

The new fifth-generation (5G) standard establishes that wireless communication systems must guarantee high transmission rates and low bit error probabilities (BEP) to support emerging communications services and applications. These requirements are essential for two 5G use cases defined as enhanced mobile broadband (eMBB) and ultra-reliable low latency communications (URLLC) [1], [2].

In wireless transmissions, the signals arrive at the receiver via different paths. As a consequence, the received signal can be randomly attenuated or amplified. This phenomenon is characterized as a random channel gain that is multiplied to the received signal. The envelope of this channel gain is known as fading. In particular, when one path, typically, the line-of-sight (LOS) path, is much stronger than the non-line-of-sight (NLOS) paths, the fading amplitude can be characterized by a Rician distribution [3]. Otherwise, when there is no a dominant path, the fading is modeled by a Rayleigh random variable.

It is well-known that fading degrades the wireless system performance. Hence, widely used techniques to counteract the undesirable fading effects are time, frequency or spatial diversity [4]–[6]. Other techniques such as error correction codes also reduce the BEP and even make it possible to obtain diversity [7]. Frequency or time diversity techniques present loss of spectral efficiency (SE) in exchange for performance improvement. Besides, opportunistic

The associate editor coordinating the review of this manuscript and approving it for publication was Junaid Nawaz Syed.

transmission (OpT) techniques have also been proposed to counteract the fading effects, which also present a loss of SE but the fading effects are mitigated in a greater extent than with the aforementioned diversity techniques [8]–[10].

With OpT, the wireless system transmits only when the instantaneous fading amplitude is above a threshold value, which is established based on a given transmission probability. If the fading amplitude is below the threshold, then the system does not transmit and symbols are stored into a buffer until the transmission is enabled again. These non-transmission periods reduce the SE. However, the good performance obtained with this technique allows the use of high order modulations, which compensates the SE reduction [11]. On the other hand, the non-transmission periods are also an interesting opportunity for cognitive networks employing the interweave technique [12], since secondary users can transmit in the non-transmission periods (white spaces) of primary users in the wireless network. OpT can also be considered as an interesting technique to provide security at the physical layer [13] because an eavesdropper does not know the transmission periods of the user in the opportunistic system, since these transmissions periods occur based on the instantaneous channel state information (CSI) of opportunistic users [14].

OpT has been exploited in sensor networks considering that each sensor, with a constrained power, must save it when its channel is highly destructive, i.e, when a low fading amplitude occurs. For example, in [8], the system performance is evaluated employing the sum rate capacity in a Rayleigh fading channel by considering that transmission is performed only when the fading has a high amplitude. The results showed that as the signal-to-noise ratio (SNR) increases, the number of active sensors is reduced due to the OpT employed. This remarkable feature reduces the probability of collisions, thereby mitigating the interference in the network. In [15], the receiver uses an antenna array and opportunism is applied because the receiver combines signals affected by fading amplitudes above a threshold value. Closed-form approximate expressions are derived for the average bit error probability (ABEP) considering a Rayleigh fading channel. The results showed that OpT outperforms the conventional[1] maximal-ratio-combining (MRC) system. Besides, the loss of SE is reduced once the use of several receiving antennas reduces the probability that the fading is below the established threshold and therefore, the non-transmission probability is very small. Besides, in [7], the performance of OpT is evaluated in encoded systems considering trellis-coded-modulation (TCM) and turbo codes are evaluated. Upper-bound expressions to evaluate the ABEP are obtained considering a Rayleigh fading channel.

OpT has also been explored in multiuser scenarios. In [16], it is analyzed by considering that each user transmits data intermittently with a certain probability (bursty transmission). For this, it is assumed an OpT based on a desired channel gain, whose envelope is modeled as a Rayleigh random variable. The authors evaluate the achievable rate under different interference conditions. The results showed that OpT achieves higher bit rate than random transmissions as well as conventional non-opportunistic transmission. Furthermore, in [9], a hybrid transmission method combining OpT and multiuser diversity is proposed. The proposed scheme considers a multiuser scenario, where only one of the users transmits based on their channel quality. ABEP expressions are derived for this scenario. In [10] and [11], co-channel interference is included and the ABEP is derived considering binary-phase-shift-keying (BPSK) modulation and square-quadrature-amplitude-modulations (S-QAM), respectively. In [17], OpT is used in a power-domain non-orthogonal multiple access (NOMA) system to reduce the interference levels in Rayleigh fading channels. An scheduling is performed based on the fading amplitude. Therefore, due to the opportunism, not all users transmit simultaneously, which reduces interference in the considered NOMA system. Moreover, the outage probability is derived. A similar scenario for opportunistic NOMA systems is assumed in [18] considering cooperative relaying. In this case, a mathematical expression to evaluate the achievable average rate in Rician fading channels is derived. In [19], it is proposed an OpT for cooperative transmissions based on the amplify and forward paradigm. Closed-form expressions to evaluate the BEP of secondary users are derived for Rayleigh fading channels. The ABEP of non-square quadrature amplitude modulations (NS-QAM) is analyzed in [20], where Rayleigh fading is considered, and the performance is evaluated via simulations for 8-QAM and 32-QAM. Square and non-square constellations are necessary for varying channel conditions and rate requirements [21]. For this reason, systems using S-QAM and NS-QAM are of great interest for wireless communications standards.

By the above and to the best of our knowledge, a study of the ABEP and the SE of opportunistic systems operating in Rician fading channels has not been conducted previously in the literature. Thus, this channel model is assumed in this work in order to evaluate the performance of opportunistic systems considering both S-QAM and NS-QAM because these modulation schemes are quite efficient in terms of spectral efficiency and energy consumption [22]. In addition, they are considered for digital broadcasting systems [23] and new generation wireless networks [24]. The main contributions of this work are summarized as follows:

- An exact single integral expression to calculate the ABEP is derived.
- A closed-form approximate ABEP expression is obtained. The exact and the approximate ABEP expressions are validated by Monte Carlo simulations considering even higher order modulations such as 1024-QAM and 2048-QAM.

[1]Henceforth, non-opportunistic transmission is called as conventional transmission.

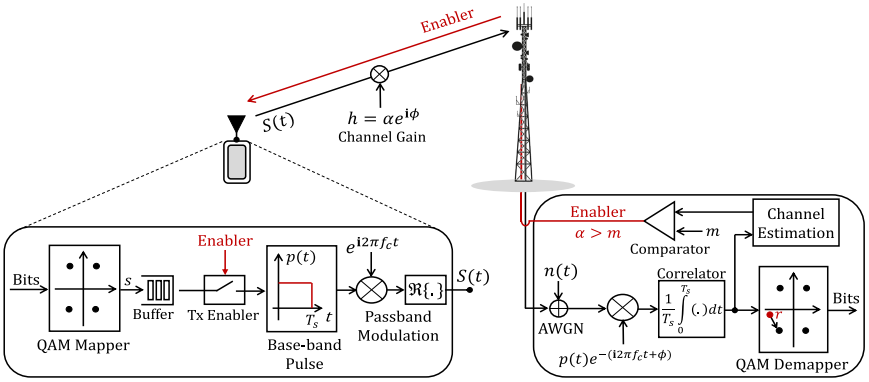

FIGURE 1. Block diagram of an opportunistic system.

- The ABEP performance considering the high SNR regime is also evaluated. For this, very simple expressions are obtained for S-QAM and NS-QAM.
- Considering a single cell scenario, an algorithm to calculate the coverage radius for each modulation is presented. The aim of this algorithm is to determine the coverage radius obtained with each modulation used in the system considering that a target ABEP must be guaranteed for the OpT.
- An expression to evaluate the mean SE is obtained considering that the Rician fading parameters change in the cellular area. This proposal allows to look for scenarios that maximize the mean SE and guarantee the target ABEP in all the cell area.

The remainder of this paper is organized as follows. The system and channel models are described in Section II. The calculation of the transmission threshold is detailed in Section III. In Section IV, expressions to evaluate the ABEP are derived. The spectral efficiency of the opportunistic system is analyzed in Section V. The numerical results and discussions are presented in Section VI. Finally, the main conclusions are presented in Section VII.

In what follows, $\Re\{\cdot\}$ represents the real part of its arguments, $(\cdot)!$ is factorial, $\lfloor\cdot\rfloor$ denotes floor operation, $\overline{x}$, $f_x(x)$ and $F_x(x)$ are the mean value, the probability density function (PDF) and the cumulative distribution function (CDF) of the random variable x, respectively. Finally, $\mathrm{P}(\cdot)$ is the probability operator and $\mathbf{i} = \sqrt{-1}$ is the imaginary unit.

II. SYSTEM AND CHANNEL MODEL

The system and channel models are described in this Section.

Fig. 1 shows the block diagram of the OpT system, where both the transmitter and the receiver employ a single antenna. In the transmitter, the bits are generated randomly with the same probability. Then, the bits are mapped into a complex symbol, s, which belong to a QAM constellation that uses Gray encoding. Thus, for a S-QAM constellation with M symbols (M-QAM), s assumes the values

$$s = [\pm(2x_1 - 1) \pm (2x_2 - 1)]A \tag{1}$$

for $x_1, x_2 \in \{1, 2, \ldots, \sqrt{M}/2\}$, where A is the signal amplitude. On the other hand, for a NS-QAM constellation with $I \times J$ symbols ($I \times J$-QAM), we have that

$$s = [\pm(2x_1 - 1) \pm (2x_2 - 1)]A \tag{2}$$

for $x_1 \in \{1, 2, \ldots, I/2\}$ and $x_2 \in \{1, 2, \ldots, J/2\}$. Notice that I and J are the order of the in-phase and quadrature pulse-amplitude-modulations (PAM) that generate the NS-QAM constellation.

The symbols are stored into a buffer until the transmission is allowed by a transmission enabler which employs the feedback link information. In opportunistic wireless systems, transmissions occur only when the fading amplitude is above a certain threshold, m [11]. For this, the receiver has knowledge of the CSI via a feedback link. The symbol at the output of the mapper takes the form of a base-band pulse format, $p(t)$, with duration T_s. This pulse format satisfies the Nyquist criterion and has unitary energy $\int_0^{T_s} p^2(t)dt = 1$. After that, the carrier with central frequency f_c is included in the base-band signal. Hence, the transmitted passband signal during a symbol interval can be written as

$$S(t) = \Re\{sp(t)\exp(\mathbf{i}\,2\pi f_c t)\}. \tag{3}$$

It is assumed that the carrier bandwidth, B, is smaller than the channel-coherence-bandwidth, which is a typical scenario for mobile wireless systems that employ orthogonal-frequency-division-multiple-access[2] (OFDMA) and that the symbol duration, T_s, is smaller than the channel-coherence-time, which is a valid assumption when the user equipment (UE) is moving at low speeds [4]. In this scenario, the channel can be modeled as frequency non-selective (flat) and slowly. Thus, considering LOS between the transmitter and the receiver, the transmitted signal is affected by a channel gain, $h = g_1 + \mathbf{i}\,g_2$, modeled by a complex Gaussian random variable, where g_1 is a zero-mean real Gaussian random variable and g_2 is a real Gaussian random variable

[2]Although the total bandwidth of the system may be greater than the channel-coherence-bandwidth, the effects of frequency selective channels are mitigated employing a cyclic prefix in OFDMA systems.

with mean value μ, such that, $\mu \neq 0$. Both g_1 and g_2 have variance σ^2. Hence, the channel gain can be also written as $h = \alpha \exp(\mathbf{i}\,\phi)$, where $\phi = \arctan(g_2/g_1)$ is a uniformly distributed random phase over $[0, 2\pi)$ and $\alpha = \sqrt{g_1^2 + g_2^2}$ is the envelope of the channel gain, that is the fading amplitude modeled by a Rician random variable, whose PDF is [25]

$$f_\alpha(\alpha) = \frac{2(K+1)}{\Omega}\alpha \exp\left(-\frac{K+1}{\Omega}\alpha^2 - K\right) \times I_0\left(2\sqrt{\frac{K(K+1)}{\Omega}}\alpha\right), \quad \alpha \geq 0, \tag{4}$$

where

$$I_0(y) = \begin{cases} 1, & y = 0, \\ \sum_{j=0}^{\infty} (j!)^{-2} \left(\frac{y}{2}\right)^{2j}, & y > 0, \end{cases} \tag{5}$$

is the modified Bessel function of the first kind and order zero [26, Eq. (9.1.10)]. Moreover,

$$K = \frac{\mu^2}{2\sigma^2}, \tag{6}$$

is the shape parameter, i.e., the ratio of the LOS path power to the remaining multipaths power, and the scale parameter

$$\Omega = \mu^2 + 2\sigma^2, \tag{7}$$

that is defined as the total power received in all paths, i.e., (7) is the mean squared fading amplitude. In the receiver, after the coherent demodulation stage and the correlator (matched filter), the received sample during a symbol interval, assuming flat fading, can be written as

$$\begin{aligned} r &= \frac{1}{T_s}\int_0^{T_s} [hS(t) + n(t)]\, p(t) \exp[-(\mathbf{i}\, 2\pi f_c t + \phi)]dt \\ &= \frac{1}{2}\alpha s + n, \end{aligned} \tag{8}$$

where we used that $h = \alpha \exp(\mathbf{i}\,\phi)$ and perfect compensation of the channel phase was also considered. The factor $1/2$ appears due to the modulation/demodulation process, α is the Rice fading amplitude, such that $\alpha > m$, and $n(t)$ is the additive white Gaussian noise (AWGN) random process. Thus, in the second step of (8), n denotes the noise sample at the matched filter output that is modeled by a zero-mean complex Gaussian random variable with variance

$$\sigma_n^2 = \frac{N_0}{2T_s}, \tag{9}$$

where N_0 is the unilateral noise power spectral density and T_s is the symbol duration.

Finally, the received sample, r, enters to a demapper, which decides on the transmitted bits.

From (8) and (9), the instantaneous signal-to-noise ratio (SNR) is obtained as

$$\gamma = \frac{\alpha^2 s^2/4}{N_0/(2T_s)} = \alpha^2 \frac{E_b}{N_0}\log_2 M, \tag{10}$$

where $P_r = s^2/2$ is the received power per symbol, $E_b = E_s/\log_2 M$ is the received bit energy, M is the modulation order and $E_s = s^2 T_s/2$ is the received energy per symbol.

Algorithm 1 Recursive Threshold Calculation

Input: q, K, Ω, δ

1: $y = \infty, m = 0$
2: **while** $y > q$ **do**
3: $\quad y = \mathcal{Q}_1\left(\sqrt{2K}, m\sqrt{\frac{2(K+1)}{\Omega}}\right)$
4: $\quad m = m + \delta$
5: **end while**
6: $m = m - \delta$

Output: m

III. TRANSMISSION THRESHOLD

In this section, the transmission threshold is calculated based on a given transmission probability. In OpT, the transmission is made when the fading amplitude is above the threshold m, then the transmission probability is obtained as

$$q = \mathrm{P}(\alpha > m) = \int_m^{\infty} f_\alpha(\alpha)d\alpha, \tag{11}$$

where $\mathrm{P}(\cdot)$ is the probability operator and $f_\alpha(\alpha)$ is given by (4). The transmission probability can be also obtained from the CDF of α, that is, $F_\alpha(\alpha)$, employing that

$$\begin{aligned} q &= 1 - F_\alpha(m) = \mathcal{Q}_1\left(\frac{\mu}{\sigma}, \frac{m}{\sigma}\right) \\ &= \mathcal{Q}_1\left(\sqrt{2K}, m\sqrt{\frac{2(K+1)}{\Omega}}\right), \end{aligned} \tag{12}$$

where

$$\mathcal{Q}_1(a, b) = \int_b^{\infty} x \exp\left(-\frac{x^2 + a^2}{2}\right) I_0(ax)dx \tag{13}$$

is the Marcum $\mathcal{Q}$-function [27] and $I_0(\cdot)$ is given by (5).

Given a transmission probability q, and the Rician parameters K and Ω, the threshold m can be obtained recursively from (12). Algorithm 1 indicates this simple procedure, where δ is an increment. Table 1 shows the threshold m as a function of the transmission probability and parameterized by the Rician factor K, where it is used that the mean power of the non-line-of-sight (NLOS) multipaths is normalized, i.e., $2\sigma^2 = 1$ (or equivalently, $\Omega = K + 1$) and $\delta = 0.0001$. In these results, notice that as q decreases, the threshold value increases, that is, the instantaneous value of the fading must be greater for the transmission to take place. As a consequence, the lower transmission probability implies in loss of SE, once the channel is not used in specific periods of time. However, it is possible to increase the modulation order to alleviate this loss and, at the same time, guarantee a good system performance. This aspect will be addressed in greater detail in Section VI.

IV. AVERAGE BIT ERROR PROBABILITY

The ABEP of OpT operating in Rician fading channels is obtained in this section for S-QAM and NS-QAM.

Let x be a random variable defined into the interval $-\infty < x < \infty$ with PDF $f_x(x)$. Suppose this random variable is

TABLE 1. Threshold m as a function of q and parameterized by the factor K.

Transmission probability, q	Rician factor K					
	0	0.5	1	2	3	4
1	0	0	0	0	0	0
3/4	0.5364	0.6809	0.8382	1.1464	1.4206	1.6638
2/3	0.6368	0.8051	0.9798	1.3040	1.5836	1.8294
1/2	0.8326	1.0434	1.2438	1.5881	1.8747	2.1239
1/3	1.0482	1.2999	1.5193	1.8770	2.1684	2.4201
2/7	1.1193	1.3832	1.6075	1.9684	2.2610	2.5134
1/4	1.1775	1.4510	1.6787	2.0420	2.3355	2.5884
1/5	1.2687	1.5564	1.7891	2.1556	2.4504	2.7039
1/6	1.3386	1.6367	1.8726	2.2413	2.5370	2.7910

conditioned to only have values between v_1 and v_2, where v_1 and v_2 are arbitrary values such that $v_1 < v_2$. This conditioned random variable has PDF $f_x(x|v_1 \le x \le v_2)$ defined into the interval $v_1 \le x \le v_2$. From [25, Section 4-4], it is known that $f_x(x|v_1 \le x \le v_2) = f_x(x)/[F_x(v_2) - F_x(v_1)]$, where $F_x(v_i)$ is the CDF of x evaluated at v_i for $i \in \{1, 2\}$.

In OpT, the system transmits only when the instantaneous fading amplitude, α, is over the threshold m, i.e. $m < \alpha < \infty$, or equivalently, $\alpha > m$. By the above, the PDF of the fading amplitude in the opportunistic transmissions is

$$f_\alpha(\alpha|\alpha > m) = \frac{f_\alpha(\alpha)}{1 - F_\alpha(m)} = \frac{f_\alpha(\alpha)}{q}, \quad \alpha > m, \tag{14}$$

where $f_\alpha(\alpha)$ and q are given by (4) and (12), respectively, and we have used that $F_\alpha(\infty) = 1$. Moreover, notice that $\int_m^\infty f_\alpha(\alpha|\alpha > m)d\alpha = 1$.

Now, let $P_b(\alpha)$ be the BEP conditioned on the instantaneous fading amplitude for the opportunistic system. Therefore, the ABEP can be calculated as follows

$$\overline{P_b} = \int_m^\infty P_b(\alpha) f_\alpha(\alpha|\alpha > m)d\alpha. \tag{15}$$

A. S-QAM

In [28, Eqs. (14),(16)], by considering the constellation symmetry of S-QAM and by assuming Gray mapping, an exact BEP expression for AWGN channels has been found, and is given as a function of the E_b/N_0 ratio and the modulation order M. From [4, Section 13.3], it is known that BEP expressions for AWGN channels can be used to calculate the instantaneous BEP in fading channels if the E_b/N_0 ratio is multiplied by the instantaneous value of the fading squared, that is, α^2. By the above, the BEP for S-QAM conditioned on the instantaneous fading amplitude can be written as

$$P_b(\alpha) = \frac{1}{\sqrt{M}\log_2\sqrt{M}} \sum_{\ell=1}^{\log_2\sqrt{M}} \sum_{\kappa=0}^{(1-2^{-\ell})\sqrt{M}-1} (-1)^{\left\lfloor \frac{\kappa 2^{\ell-1}}{\sqrt{M}} \right\rfloor} \times \left(2^{\ell-1} - \left\lfloor \frac{\kappa 2^{\ell-1}}{\sqrt{M}} + \frac{1}{2} \right\rfloor\right) \operatorname{erfc}\left[\sqrt{\alpha^2\, \zeta_\kappa\left(M, \frac{E_b}{N_0}\right)}\right], \tag{16}$$

where $\lfloor y \rfloor$ denotes the floor operation, which returns the greatest integer that is smaller than or equal to y and $\operatorname{erfc}(\cdot)$ is the complementary error function given by [25]

$$\operatorname{erfc}(y) = \frac{2}{\sqrt{\pi}} \int_y^\infty \exp(-w^2)dw, \tag{17}$$

and

$$\zeta_\kappa\left(M, \frac{E_b}{N_0}\right) = \frac{3(2\kappa+1)^2}{2(M-1)} \frac{E_b}{N_0} \log_2 M. \tag{18}$$

From (12)-(16), the ABEP for opportunistic systems operating in Rician fading channels ($K > 0$) is calculated as

$$\overline{P_b} = \frac{1}{\sqrt{M}\log_2\sqrt{M}} \sum_{\ell=1}^{\log_2\sqrt{M}} \sum_{\kappa=0}^{(1-2^{-\ell})\sqrt{M}-1} (-1)^{\left\lfloor \frac{\kappa 2^{\ell-1}}{\sqrt{M}} \right\rfloor} \times \left(2^{\ell-1} - \left\lfloor \frac{\kappa 2^{\ell-1}}{\sqrt{M}} + \frac{1}{2} \right\rfloor\right) \times \frac{1}{q} \int_m^\infty \operatorname{erfc}\left[\sqrt{\alpha^2\, \zeta_\kappa\left(M, \frac{E_b}{N_0}\right)}\right] f_\alpha(\alpha)d\alpha, \tag{19}$$

Now, replacing $f_\alpha(\alpha)$ given by (4), and by employing the definition of the modified Bessel function given by (5) on this PDF,[3] we obtain after some manipulations that

$$\overline{P_b} = \frac{2(K+1)\exp(-K)}{q\Omega\sqrt{M}\log_2\sqrt{M}} \sum_{\ell=1}^{\log_2\sqrt{M}} \sum_{\kappa=0}^{(1-2^{-\ell})\sqrt{M}-1} (-1)^{\left\lfloor \frac{\kappa 2^{\ell-1}}{\sqrt{M}} \right\rfloor} \times \left(2^{\ell-1} - \left\lfloor \frac{\kappa 2^{\ell-1}}{\sqrt{M}} + \frac{1}{2} \right\rfloor\right) \sum_{j=0}^{\infty} \left[\frac{K(K+1)}{\Omega}\right]^j \frac{\mathcal{I}_j}{(j!)^2}, \tag{20}$$

where $\mathcal{I}_j$ is an integral defined as

$$\mathcal{I}_j = \int_m^\infty \alpha^{2j+1} \exp\left(-\alpha^2 \frac{K+1}{\Omega}\right) \times \operatorname{erfc}\left[\sqrt{\alpha^2\, \zeta_\kappa\left(M, \frac{E_b}{N_0}\right)}\right] d\alpha. \tag{21}$$

Unfortunately, (21) cannot be evaluated in closed-form in terms of elementary functions. However, an approximation can be obtained. Notice that (17) can be rewritten as a series by using integration by parts. For this, we first rewrite (17) as

$$\operatorname{erfc}(y) = \frac{2}{\sqrt{\pi}} \int_y^\infty w^{-1} \exp(-w^2) w\, dw. \tag{22}$$

Let $u = w^{-1}$, $du = -w^{-2}$, $dv = \exp(-w^2)wdw$ and $v = -\exp(-w^2)/2$. Hence,

$$\operatorname{erfc}(y) = \frac{2}{\sqrt{\pi}} \left[uv\Big|_y^\infty - \int_y^\infty v du\right]$$

[3]Notice that we considered the scenario $y > 0$ in (5). This is because the argument of $I_0(\cdot)$ in (4) is always greater than zero because $\alpha > m$ for OpT, and $K > 0$, $\Omega > 0$ for Rician fading.

$$= \frac{2}{\sqrt{\pi}}\left[\frac{1}{2y}\exp\left(-y^2\right) - \frac{1}{2}\underbrace{\int_y^\infty \frac{1}{w^3}\exp\left(-w^2\right)wdw}_{\mathcal{J}}\right]. \quad (23)$$

Similarly, notice that $\mathcal{J}$ in (23) can be integrated by parts using $u = 1/w^3$, $du = -3w^{-4}$, $dv = \exp(-w^2)wdw$ and $v = -\exp(-w^2)/2$. Hence,

$$\mathcal{J} = \frac{1}{2y^3}\exp\left(-y^2\right) - \frac{3}{2}\int_y^\infty \frac{1}{w^5}\exp\left(-w^2\right)wdw. \quad (24)$$

With (23) and (24), (22) is rewritten as

$$\operatorname{erfc}(y) = \frac{1}{\sqrt{\pi}}\left[\frac{1}{y}\exp\left(-y^2\right) - \frac{1}{2y^3}\exp\left(-y^2\right) + \frac{3}{2}\int_y^\infty \frac{1}{w^5}\exp\left(-w^2\right)wdw\right]. \quad (25)$$

Thus, repeating the previous process an infinite number of times yields

$$\operatorname{erfc}(y) = \frac{\exp\left(-y^2\right)}{y\sqrt{\pi}}\left[1+\sum_{\kappa=1}^{\infty}\frac{1\times 3\times 5\times\cdots\times(2\kappa-1)}{(-2y^2)^\kappa}\right]. \quad (26)$$

For large y, only the first term in the above series is dominant. Therefore, we can consider it in order to derive an approximation for the complementary error function, that is, $\operatorname{erfc}(y) \approx (y\sqrt{\pi})^{-1}\exp(-y^2)$. Fig. 2 shows the exact $\operatorname{erfc}(x)$ and the proposed approximation. These results show the closeness of the approximation.

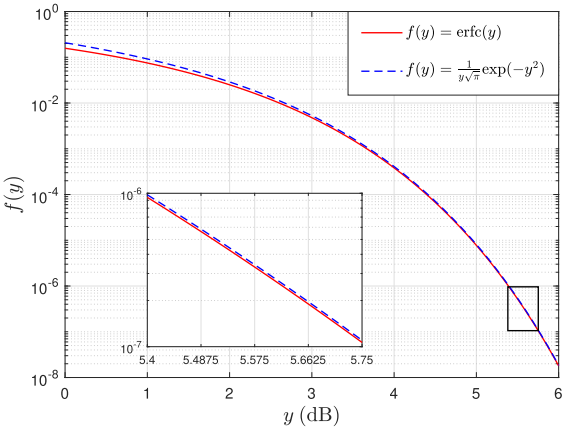

FIGURE 2. Complementary error function approximation.

With the above result, an approximation for (21) is determined. Hence, it is possible to approximate (21) employing elementary functions as

$$\mathcal{I}_j \approx \frac{1}{2}\left[\pi\zeta_\kappa\left(M,\frac{E_b}{N_0}\right)\right]^{-\frac{1}{2}}\left[\zeta_\kappa\left(M,\frac{E_b}{N_0}\right)+\frac{K+1}{\Omega}\right]^{-j-\frac{1}{2}} \times\Gamma\left\{j+\frac{1}{2},m^2\left[\zeta_\kappa\left(M,\frac{E_b}{N_0}\right)+\frac{K+1}{\Omega}\right]\right\}, \quad (27)$$

where

$$\Gamma(a,y) = \int_y^\infty u^{a-1}\exp(-u)du \quad (28)$$

is the incomplete gamma function [29, eq. (8.350.1)]. Thus, replacing (27) in (20), we obtain an approximate expression to evaluate the ABEP of opportunistic systems operating with S-QAM in Rician fading channels, given by

$$\overline{P_b} \approx \frac{(K+1)\exp(-K)}{q\Omega\sqrt{\pi M}\log_2\sqrt{M}}\sum_{\ell=1}^{\log_2\sqrt{M}}\sum_{\kappa=0}^{(1-2^{-\ell})\sqrt{M}-1}(-1)^{\left\lfloor\frac{\kappa 2^{\ell-1}}{\sqrt{M}}\right\rfloor} \times\left(2^{\ell-1}-\left\lfloor\frac{\kappa 2^{\ell-1}}{\sqrt{M}}+\frac{1}{2}\right\rfloor\right)\sum_{j=0}^{\mathcal{T}}\left[\frac{K(K+1)}{\Omega}\right]^j\frac{1}{(j!)^2} \times\left[\zeta_\kappa\left(M,\frac{E_b}{N_0}\right)\right]^{-\frac{1}{2}}\left[\zeta_\kappa\left(M,\frac{E_b}{N_0}\right)+\frac{K+1}{\Omega}\right]^{-j-\frac{1}{2}} \times\Gamma\left\{j+\frac{1}{2},m^2\left[\zeta_\kappa\left(M,\frac{E_b}{N_0}\right)+\frac{K+1}{\Omega}\right]\right\}. \quad (29)$$

Notice that the upper limit of the last summation has been replaced by $\mathcal{T}\in\mathbb{Z}^+$. From (5), the exact calculation of the modified Bessel function is obtained when $\mathcal{T}$ goes to infinity. However, it is possible to reduce the evaluation complexity by using a $\mathcal{T}$ much less than infinity and still guarantee an adequate accuracy. This aspect is validated in Section VI.

For the particular case of Rayleigh fading ($K = 0$), from (5), the above expression can be rewritten as

$$\overline{P_b} \approx \frac{1}{q\Omega\sqrt{\pi M}\log_2\sqrt{M}}\sum_{\ell=1}^{\log_2\sqrt{M}}\sum_{\kappa=0}^{(1-2^{-\ell})\sqrt{M}-1}(-1)^{\left\lfloor\frac{\kappa 2^{\ell-1}}{\sqrt{M}}\right\rfloor} \times\left(2^{\ell-1}-\left\lfloor\frac{\kappa 2^{\ell-1}}{\sqrt{M}}+\frac{1}{2}\right\rfloor\right)\left[\zeta_\kappa\left(M,\frac{E_b}{N_0}\right)\right]^{-\frac{1}{2}} \times\left[\zeta_\kappa\left(M,\frac{E_b}{N_0}\right)+\frac{1}{\Omega}\right]^{-\frac{1}{2}}\Gamma\left\{\frac{1}{2},m^2\left[\zeta_\kappa\left(M,\frac{E_b}{N_0}\right)+\frac{1}{\Omega}\right]\right\}. \quad (30)$$

Next, we simplify (29) by considering the high SNR regime, i.e., when E_b/N_0 goes to infinity. In this case, it can be shown that the most significant term in the last summation of (29) appears when $j = 0$. Moreover, from [29, eqs. (8.250.1), (8.250.4), (8.359.3)], it is obtained that $\Gamma(1/2,y) = \sqrt{\pi}\operatorname{erfc}(\sqrt{y})$. In addition, using again that $\operatorname{erfc}(y) \approx (y\sqrt{\pi})^{-1}\exp(-y^2)$, and that $\zeta_\kappa(M,E_b/N_0) \gg (K+1)/\Omega$, we can simplify (29) as

$$\overline{P_b} \approx \frac{(K+1)\exp(-K)}{q\Omega m\sqrt{\pi M}\log_2\sqrt{M}}\sum_{\ell=1}^{\log_2\sqrt{M}}\sum_{\kappa=0}^{(1-2^{-\ell})\sqrt{M}-1}(-1)^{\left\lfloor\frac{\kappa 2^{\ell-1}}{\sqrt{M}}\right\rfloor} \times\left(2^{\ell-1}-\left\lfloor\frac{\kappa 2^{\ell-1}}{\sqrt{M}}+\frac{1}{2}\right\rfloor\right)\frac{\exp\left[-m^2\zeta_\kappa(M,E_b/N_0)\right]}{[\zeta_\kappa(M,E_b/N_0)]^{3/2}}, \quad (31)$$

which is valid for any $K \geq 0$.

B. NS-QAM

In [28, Eqs. (20)-(22)], it was found an exact BEP expression for NS-QAM in AWGN channels. In particular, for any $I \times J$-QAM modulation. Thus, by following the guidelines of [4, Section 13.3], these expressions can be employed to calculate the instantaneous BEP in fading channels if the E_b/N_0 ratio is multiplied by α^2. Hence, the BEP expression conditioned on the instantaneous fading amplitude is

$$P_b(\alpha) = \frac{1}{\log_2(IJ)} \left[\sum_{\ell=1}^{\log_2 I} \mathcal{P}_{I,\ell}(\alpha) + \sum_{\ell=1}^{\log_2 J} \mathcal{P}_{J,\ell}(\alpha) \right], \quad (32)$$

with

$$\mathcal{P}_{W,\ell}(\alpha) = \frac{1}{W} \sum_{\kappa=0}^{(1-2^{-\ell})w-1} (-1)^{\left\lfloor \frac{\kappa 2^{\ell-1}}{W} \right\rfloor} \left(2^{\ell-1} - \left\lfloor \frac{\kappa 2^{\ell-1}}{W} + \frac{1}{2} \right\rfloor \right) \times \operatorname{erfc}\left[\sqrt{\alpha^2 \, \rho_\kappa \left(I, J, \frac{E_b}{N_0} \right)} \right], \quad (33)$$

for $W \in \{I, J\}$ and

$$\rho_\kappa \left(I, J, \frac{E_b}{N_0} \right) = \frac{3(2\kappa+1)^2}{I^2 + J^2 - 2} \frac{E_b}{N_0} \log_2(IJ), \quad (34)$$

From (15) and (14), the exact ABEP of OpTs operating with NS-QAM in Rician fading channels is given by

$$\overline{P_b} = \frac{1}{q \log_2(IJ)} \left[\sum_{\ell=1}^{\log_2 I} \int_m^\infty \mathcal{P}_{I,\ell}(\alpha) f_\alpha(\alpha) d\alpha + \sum_{\ell=1}^{\log_2 J} \int_m^\infty \mathcal{P}_{J,\ell}(\alpha) f_\alpha(\alpha) d\alpha \right], \quad (35)$$

where $f_\alpha(\alpha)$ is given by (4).

Following the same procedure of previous subsection, it is possible to determine that (35) can be approximated by

$$\overline{P_b} \approx \frac{1}{q\Omega\sqrt{\pi} \log_2(IJ)} \left[\sum_{\ell=1}^{\log_2 I} \overline{\mathcal{P}_{I,\ell}} + \sum_{\ell=1}^{\log_2 J} \overline{\mathcal{P}_{J,\ell}} \right], \quad (36)$$

where $\overline{P_{W,\ell}}$ for $W \in \{I, J\}$ and for $K > 0$ is given by (37), located as shown at the bottom of the next page. In particular, for Rayleigh fading ($K = 0$), that expression can be rewritten as

$$\overline{P_{W,\ell}} \approx \frac{1}{W} \sum_{\kappa=0}^{(1-2^{-\ell})\sqrt{M}-1} (-1)^{\left\lfloor \frac{\kappa 2^{\ell-1}}{\sqrt{M}} \right\rfloor} \left(2^{\ell-1} - \left\lfloor \frac{\kappa 2^{\ell-1}}{\sqrt{M}} + \frac{1}{2} \right\rfloor \right) \times \left[\rho_\kappa \left(I, J, \frac{E_b}{N_0} \right) \right]^{-\frac{1}{2}} \left[\rho_\kappa \left(I, J, \frac{E_b}{N_0} \right) + \frac{1}{\Omega} \right]^{-j-\frac{1}{2}} \times \Gamma \left\{ \frac{1}{2}, m^2 \left[\rho_\kappa \left(I, J, \frac{E_b}{N_0} \right) + \frac{1}{\Omega} \right] \right\}. \quad (38)$$

Finally, (37) can be simplified at the high SNR regime by taken the most significant term in the last summation ($j = 0$), employing that $\Gamma(1/2, y) = \sqrt{\pi} \operatorname{erfc}(\sqrt{y})$, that $\operatorname{erfc}(y) \approx (y\sqrt{\pi})^{-1} \exp(-y^2)$, and that $\rho_\kappa (I, J, E_b/N_0) \gg (K+1)/\Omega$. Therefore, (37) can be simplified as

$$\overline{P_{W,\ell}} \approx \frac{(K+1)\exp(-K)}{q\Omega m W \sqrt{\pi}} \sum_{\kappa=0}^{(1-2^{-\ell})\sqrt{M}-1} (-1)^{\left\lfloor \frac{\kappa 2^{\ell-1}}{\sqrt{M}} \right\rfloor} \times \left(2^{\ell-1} - \left\lfloor \frac{\kappa 2^{\ell-1}}{\sqrt{M}} + \frac{1}{2} \right\rfloor \right) \frac{\exp\left[-m^2 \rho_\kappa (I, J, E_b/N_0) \right]}{\left[\rho_\kappa (\kappa, I, J, E_b/N_0) \right]^{3/2}}, \quad (39)$$

which is valid for any $K \geq 0$. From (31) and (39), notice that the ABEP decays exponentially when the SNR increases. This implies that the fading effects are highly mitigated as a consequence of OpT.[4] Besides, the higher the threshold m, the faster the ABEP decays as SNR increases. Finally, as K increases, the ABEP is reduced by a factor $(K+1)\exp(-K)$.

V. SPECTRAL EFFICIENCY

The SE, ξ, is defined as the ratio between the bit rate, R_b, and the bandwidth employed, B. From Nyquist theorem, the maximum achievable bit rate is $R_b = B \log_2 M$. As a consequence, for a given modulation M, the SE is $\xi = \log_2 M$ bits/s/Hz. Once the channel is not occupied all the time in OpT, the SE can be rewritten as

$$\xi = q \log_2 M \quad \text{bits/s/Hz}, \quad (40)$$

where q is the transmission probability given by (12).

In a real scenario, it is adequate to calculate the mean SE considering the distance between the UE and the base station (BS) once the channel conditions may change into the cell area [30]. For this analysis, in the following we consider a circular cell with an internal radius[5] R_0, an external radius R and a BS at the cell center, as shown in Fig. 3, where r is the distance between the UE and the BS and θ is the angle between the user position and the horizontal axis. In Fig. 3, we have considered that the Rician parameters K and Ω change within the cell. For example, for a distance $\wp_2 \leq r \leq \wp_3$, the Rician parameters are K_3 and Ω_3. Thus, for simplicity, we assume that the Rician parameters change according to $\mathcal{C}$ concentric rings ($\mathcal{C} = 4$ in Fig. 3). In addition, we assume that the system uses $\mathcal{N}$ different modulations ($\mathcal{N} = 4$ in Fig. 3). Hence, $\mathcal{R}_\kappa$ is the coverage radius obtained with the modulation M_κ for $\kappa \in \{1, 2, \ldots, \mathcal{N}\}$.

We also assume that user location is uniformly distributed in the cell area, i.e., there is the same probability that the user is in any part of the cell. Consequently, we can write that the cell area, a, is a uniformly distributed random variable with PDF $f_a(a) = [2\pi(R^2 - R_0^2)]^{-1}$ for $2\pi R_0^2 \leq a \leq 2\pi R^2$. Hence,

[4] In conventional wireless transmissions, the ABEP decays linearly as the SNR increases. In conventional AWGN transmissions, the ABEP decays exponentially as the SNR increases. This behavior is noticed in the BER expressions for AWGN channels in which the complementary error function generally appears [22] (Refer to eq. (26)).

[5] The circular cell with a small hole at the center ensures convergence in the average received power at the BS.

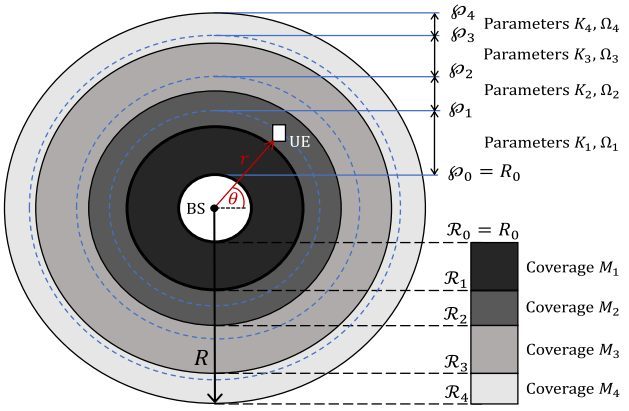

FIGURE 3. Cell coverage radii for different modulation schemes.

applying a simple transformation of random variables, we can determine that the PDF of r is given by

$$f_r(r) = \frac{2r}{R^2 - R_0^2}, \quad R_0 \leq r \leq R, \tag{41}$$

and the PDF of θ is given by

$$f_\theta(\theta) = \frac{1}{2\pi}, \quad 0 \leq \theta < 2\pi. \tag{42}$$

From (40)-(42), the mean SE can be calculated as

$$\begin{aligned}\overline{\xi} &= \int_0^{2\pi} \int_{R_0}^{R} q \log_2 M(r) f_r(r) f_\theta(\theta) dr d\theta \\ &= q \sum_{\kappa=0}^{\mathcal{N}-1} \frac{(\mathcal{R}_{\kappa+1} - \mathcal{R}_\kappa)}{R^2 - R_0^2} \log_2 (M_{\kappa+1}),\end{aligned} \tag{43}$$

where $M(r)$ is the modulation employed as a function of the distance between the UE and the BS.

By the above, the mean SE depends on the coverage radius for each modulation. For the calculation of these radii, we consider that a target ABEP, $P_{b,t}$, must be guaranteed for the UE in any cell region. Algorithm 2 calculates the coverage radii employing the expressions derived in Section IV. The algorithm requires some input parameters as the target ABEP, $P_{b,t}$, the UE maximum transmission power, $P_{t,m}$, the noise power spectral density, N_0, the internal cell radius, R_0, the external cell radius, R, the transmission probability, q, the Rician parameters $K(r)$ and $\Omega(r)$ as a function of the distance between the UE and the BS, and the modulations used in the system, which are into the vector $\vec{M} = [M_1, M_2, \ldots M_{\mathcal{N}}]$, such that $M_1 > M_2 > \ldots > M_{\mathcal{N}}$, the value δ_1 is an E_b/N_0 increment, and δ_2 is an increment for r in meters.

In Algorithm 2, mod$(y, 2)$ calculates modulo 2 operation with the argument y. Thus, if mod$(\log_2 M_\kappa, 2)$ is equal to zero, then M_κ is S-QAM, otherwise, it is NS-QAM. For each modulation, the algorithm calculates ζ_k, given by (18), for S-QAM or ρ_k, given by (34), for NS-QAM, as appropriate, which remain as a function of E_b/N_0 (steps 5 to 9). Then, the E_b/N_0 required to ensure the target ABEP is obtained recursively from (29) or (36), as appropriate (steps 11 to 18). The received power at the BS is obtained in step 19, where it is used that $R_b = B \log_2 M$, $E_s = E_b \log_2 M$ and that the received power is $P_r = s^2/2$. In order to obtain the coverage radius for the current modulation, the distance r is varied from R_0 to R with increments of δ_2.

An efficient way to use the power resources in the UE is employing power control. Moreover, since the aim is to guarantee the received power P_r obtained in step 19 of Algorithm 2, there is no reason for the received power to be greater than P_r. Therefore, the closer the UE is to the BS, the lower the transmission power. While the UE is more distant from the BS, it increases the transmission power to ensure P_r, but the power can only be increased up to $P_{t,m}$. If this limit is reached, the UE must decrease the modulation order to guarantee the target ABEP. As a consequence of the path-loss, the received power can be written as $P_r = \mathcal{P} P_t r^{-\beta}$, where $\mathcal{P}$ and β are the path-loss factor and the path-loss exponent, respectively. From this analysis, the transmission power necessary to guarantee P_r is calculated in steps 20 to 23 in the algorithm. The $\mathcal{P}$ and β parameters depend on the propagation model used. In this work, the Stanford University Interim (SUI) path-loss model is adopted because it considers the 3.5 GHz band, which is a candidate for 5G networks deployment [32]. With this model, r satisfies that 100 m $\leq r \leq$ 10000 m and from [31], we have that

$$\mathcal{P} = \frac{5625}{\pi^2} 2000^x f_c^{-(2+x)} 100^{\beta-2} \left(\frac{h_u}{2}\right)^{0.1y}, \tag{44}$$

$$\beta = z_1 - z_2 h_a + \frac{z_3}{h_a}, \tag{45}$$

where $f_c \leq 3500$ MHz, h_a and h_u are the BS antenna height and the UE height in meters, respectively, such that 10 m $\leq h_a \leq$ 80 m and 1 m $\leq h_u \leq$ 10 m. Moreover, $x = 0.6$ for $f_c \geq$ 2000 MHz, otherwise, $x = 0$, y is equal to 0 for $h_u < 2$ m, otherwise, $y = 10.8$ is employed for heavy urban path-loss conditions. In these conditions, $z_1 = 4.6$, $z_2 = 0.0075$ and $z_3 = 12.6$ are also used. Other values for these constants are available in [31] for different path-loss environments.

$$\begin{aligned}\overline{P_{W,\ell}} \approx \frac{(K+1)\exp(-K)}{W} \sum_{\kappa=0}^{(1-2^{-\ell})\sqrt{M}-1} (-1)^{\left\lfloor \frac{\kappa 2^{\ell-1}}{\sqrt{M}} \right\rfloor} \left(2^{\ell-1} - \left\lfloor \frac{\kappa 2^{\ell-1}}{\sqrt{M}} + \frac{1}{2} \right\rfloor\right) \sum_{j=0}^{\mathcal{T}} \left[\frac{K(K+1)}{\Omega}\right]^j \frac{1}{(j!)^2} \\ \times \left[\rho_\kappa\left(I, J, \frac{E_b}{N_0}\right)\right]^{-\frac{1}{2}} \left[\rho_\kappa\left(I, J, \frac{E_b}{N_0}\right) + \frac{K+1}{\Omega}\right]^{-j-\frac{1}{2}} \Gamma\left\{j + \frac{1}{2}, m^2\left[\rho_\kappa\left(I, J, \frac{E_b}{N_0}\right) + \frac{K+1}{\Omega}\right]\right\}\end{aligned} \tag{37}$$

Algorithm 2 Coverage Radii Calculation

Input: $P_{b,t}, P_{t,m}, N_0, R_0, R, q, K(r), \Omega(r)$, $\vec{M} = [M_1, M_2, \ldots M_{\mathcal{N}}], \delta_1, \delta_2$

for $\ell = 1$ **to** $\mathcal{C}$ **do**
  $r = \wp_\ell$
  Calculate m using Algorithm 1 with $K(r)$ and $\Omega(r)$
  for $\kappa = 1$ **to** $\mathcal{N}$ **do**
    if $\text{mod}(\log_2 M_\kappa, 2) = 0$ **then**
      Obtain ζ_k as a function of E_b/N_0 employing (18)
    else
      Obtain ρ_k as a function of E_b/N_0 employing (34)
    end if
    $\overline{P_b} = P_{b,t}, E_b/N_0 = 0$
    while $\overline{P_b} \geq P_{b,t}$ **do**
      if $\text{mod}(\log_2 M_\kappa, 2) = 0$ **then**
        Evaluate (29) with M_κ, q, m, $K(r)$, $\Omega(r)$ and the current value of E_b/N_0
      else
        Evaluate (36) with M_κ, q, m, $K(r)$, $\Omega(r)$ and the current value of E_b/N_0
      end if
      $E_b/N_0 = E_b/N_0 + \delta_1$
    end while
    $P_r = N_0 R_b E_b/N_0, P_t = 0$
    while $r \leq \wp_\ell$ **and** $P_t \leq P_{t,m}$ **do**
      $r = r + \delta_2$
      $P_t = \mathcal{P}^{-1} P_r r^\beta$
    end while
    $\mathcal{R}_\kappa = r$
  end for
end for

Output: $\mathcal{R}_1, \mathcal{R}_2, \ldots, \mathcal{R}_{\mathcal{N}}$

In algorithm 2, $P_t = P_{t,m}$, for a given r, that value of r is the coverage radius for the current modulation, i.e., $\mathcal{R}_\kappa = r$. Finally, if all modulations have been used and if $r > \wp_\mathcal{C}$, where $\wp_\mathcal{C} = R$ (refer to Fig. 3), the algorithm ends. The outputs are the coverage radii for all modulations.

VI. NUMERICAL RESULTS

The system performance is evaluated in this section employing our derived expressions in some scenarios. The theoretical analysis accuracy is validated using Monte Carlo simulations. For simulation purposes, the mean power of the QAM constellations have been normalized, i.e, the signal amplitude A has been selected so that $\overline{s^2} = 1$, the mean power of the NLOS paths has also been normalized, i.e., $2\sigma^2 = 1$, and the threshold values in Table 1 are employed.

Fig. 4 and Fig. 5 show the ABEP as a function of the normalized SNR, E_b/N_0, parameterized by the modulation order considering S-QAM and NS-QAM, respectively. Both figures consider a Rician factor $K = 1$, a transmission probability $q = 1/3$ and $\mathcal{T} = 8$ terms are employed to obtain the approximate ABEP expression (eq. (29) for Fig. 4, eq. (36) for Fig. 5). Moreover, the exact ABEP is plotted along with the approximate ABEP expression derived for high SNR. In the figures, notice the accuracy of the derived expressions with the simulations results. The approximate expression is highly accurate in all the SNR regime for low modulation orders, but, as the modulation order increases, it is accurate at high SNR and becomes an upper-bound for low SNR, which is more evident for high order modulations like 256-QAM, 512-QAM, 1024-QAM and 2048-QAM. On the other hand, the expression derived for the high SNR regime follows the exact curves decayment as the SNR increases. As expected, as M increases, the ABEP increases for a given E_b/N_0. In addition, observe that OpT allows an exponential decayment of the ABEP curves when they are plotted as a function of the SNR, once the ABEP curves decay linearly as the SNR (in dB) increases in conventional transmissions [33]. This particular behavior is observed later in Fig. 8.

Fig. 6 shows the ABEP as a function of the E_b/N_0, parameterized by the Rician K factor and the modulation order considering a transmission probability $q = 2/3$ and $\mathcal{T} = 8$

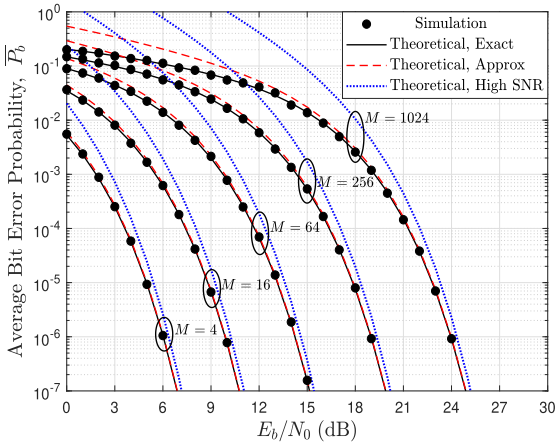

FIGURE 4. ABEP as a function of the E_b/N_0, parameterized by the modulation order considering S-QAM, $K = 1$, $q = 1/3$ and $\mathcal{T} = 8$.

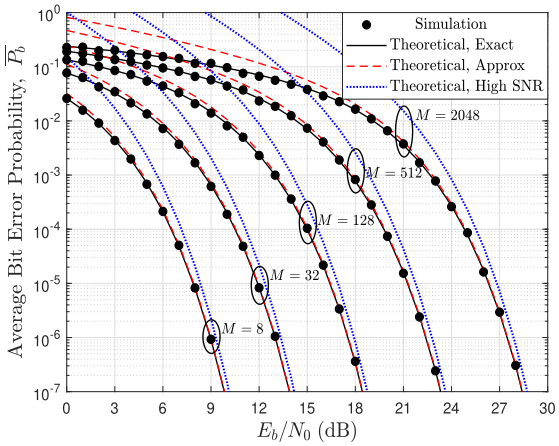

FIGURE 5. ABEP as a function of the E_b/N_0, parameterized by the modulation order considering NS-QAM, $K = 1$, $q = 1/3$ and $\mathcal{T} = 8$.

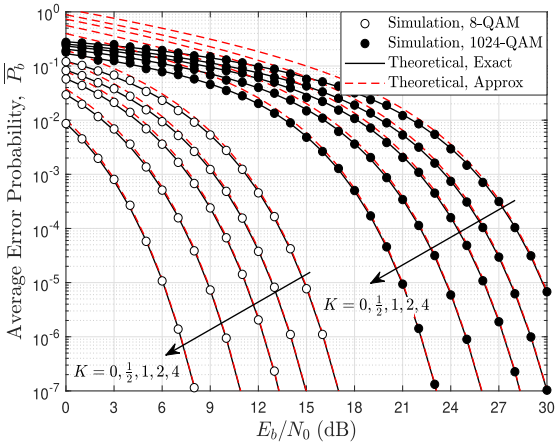

FIGURE 6. ABEP as a function of the E_b/N_0, parameterized by the Rician K factor and the modulation order considering $q = 2/3$ and $\mathcal{T} = 8$.

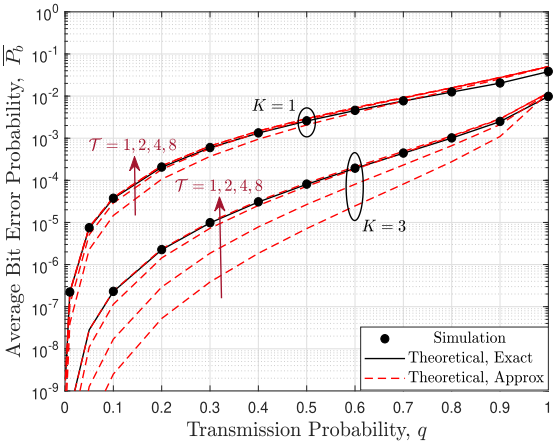

FIGURE 7. ABEP as a function of the transmission probability q, parameterized by the Rician K factor and $\mathcal{T}$ considering 64-QAM and $E_b/N_0 = 10$ dB.

terms for obtaining the approximate theoretical ABEP curve. We have considered a very low and a very high QAM modulation to observe the effects of the Rician K factor on the system performance. Observe that as K increases the BER is improved. It is interesting to notice that similar improvements in terms of the SNR are obtained for 8-QAM and 1024-QAM. As an example, when K increases from 0 to 2, there is an E_b/N_0 gain of 6.92 dB for 8-QAM and a gain of 6.90 dB for 1024-QAM when $\overline{P_b} = 10^{-7}$. Notice also that the K factor has a great impact in the opportunistic system performance. Thus, comparing 8-QAM with $K = 0$, and 1024-QAM with $K = 4$, notice that 1024-QAM requires only 6.1 dB more SNR than 8-QAM to guarantee $\overline{P_b} = 10^{-7}$. Obviously, it is important to remember that the K factor depends on the position of the transmitter in relation to the receiver [34]. Moreover, from (40), the SE of the opportunistic system using 8-QAM is $\xi = \frac{2}{3}\log_2(8) = 2$ bits/s/Hz and the SE of the opportunistic system using 1024-QAM is $\xi = \frac{20}{3} \approx 6.67$ bits/s/Hz. By the above, OpT reduce the SE by a factor of q, but, due to the impressive performance gain, it is possible to use very high modulations and still guarantee a low ABEP with reasonable values of SNR.

Fig. 7 shows the ABEP as a function of the transmission probability q, parameterized by the Rician K factor and $\mathcal{T}$ considering 64-QAM and $E_b/N_0 = 10$ dB. Simulation results are obtained for $\overline{P_b} \geq 10^{-7}$. As the transmission probability increases, the threshold m is reduced. This aspect can be observed in Table 1, and implies that the fading amplitude values considered to perform the OpT decrease. Therefore, the signal may be attenuated by the fading channel, and the noise effects impair the system performance to a greater extent. Consequently, we observe that as q increases, the ABEP increases too. In particular, when $q = 1$, OpT becomes a conventional transmission, that is, the system transmits all the time. Moreover, it can be noticed again that as K increases, the system performance improves. Another key aspect to be noted in this figure is the accuracy of the theoretical approximate ABEP expression. Observe that for $\mathcal{T} = 1$, there is a significant difference between the exact results and the approximate ABEP curve. However, as $\mathcal{T}$ increases, the approximation becomes more accurate. Thus, with only $\mathcal{T} = 8$ terms in the last summation of (29) or (37), as appropriate, we obtain accurate closed-form expressions to evaluate the ABEP of the opportunistic system. Last, note there is a small difference between the exact theoretical curve and the approximated ones in the high ABEP region. This occurs due to the approximations made in the theoretical analysis and this difference is also observed in previous figures. The way to mitigate this difference is by increasing the value of $\mathcal{T}$. However, the high ABEP region is not usually of interest. Therefore, small values of $\mathcal{T}$ already offer adequate accuracy for the analysis of the opportunistic system. On the other hand, it is important to indicate that this small difference between exact and approximate theoretical results decreases as the E_b/N_0 is increased.

Fig. 8 shows the ABEP as a function of the E_b/N_0, parameterized by the modulation order, $K = 2$ and $\mathcal{T} = 8$. The transmission probability employed for each modulation is $q = 2/\log_2 M$, as a consequence, the SE for all the scenarios is $\xi = q\log_2 M = 2$ bits/s/Hz. In the particular case of 4-QAM ($M = 4$), we have that $q = 1$, which corresponds to the conventional transmission, hence, the ABEP curves decay linearly. Therefore, as the SNR increases, notice that OpT guarantees a lower ABEP than the conventional transmission even with the same SE. Observe that 16-QAM ensures a lower ABEP than 8-QAM. This result may seem strange but it is important to remember that both scenarios have the same SE. In addition, it is known that 8-QAM performs better than 16-QAM in conventional transmissions, but there is no relatively high gain in terms of SNR (about 0.6 dB in Rayleigh fading channels). Moreover, from Table 1, we have that $m = 1.3018$ for $q = 2/3$ and $m = 1.5881$ for $q = 1/2$. Thus, 16-QAM transmissions are made when higher fading amplitudes occur. Thus, OpT generates this interesting and atypical

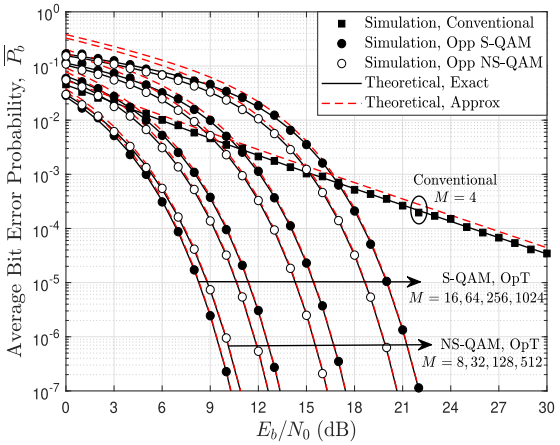

FIGURE 8. ABEP as a function of the E_b/N_0, parameterized by the modulation order considering some scenarios with SE $\xi = 2$ bits/s/Hz, $K = 2$ and $\mathcal{T} = 8$.

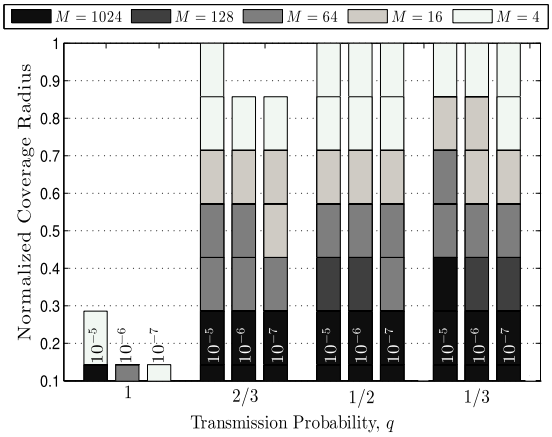

FIGURE 9. Normalized coverage radii as a function of the transmission probability, q, and parameterized by the target ABEP, $P_{b,t}$.

result. Ignoring this particular case, it is observed that as the modulation order increases, the system performance worsens despite the same SE is maintained. Therefore, the transmission probability and the modulation must be chosen so that the best system performance is guaranteed.

In the following, the mean SE is evaluated. For this, we consider a scenario similar to that of Fig. 3, where a circular cell, with internal radius $R_0 = 100$ m and external radius $R = 1400$ m, is divided into concentric rings, and the Rician parameters are different in each ring. The channel parameters are detailed in Table 2 as a function of the distance between the UE and the BS. In addition, it is assumed an opportunistic system operating in the central frequency $f_c = 3.5$ GHz and employing 1024-QAM, 128-QAM, 64-QAM, 16-QAM and 4-QAM modulations in an urban scenario with heavy path-loss conditions.[6] The BS antenna height and the UE antenna height are set to $h_a = 30$ m and $h_u = 1.6$ m, respectively. Finally, some parameters from the 5G Release 15 standard are used: a maximum UE transmission power $P_{t,m} = 23$ dBm [35], a carrier bandwidth $B = 15$ kHz [36], and a noise power spectral density $N_0 = 4.004 \times 10^{-21}$ Watts/Hz.

Fig. 9 shows the normalized coverage radii as a function of the transmission probability, q, and parameterized by the target ABEP, $P_{b,t}$ considering the scenarios of Table 2. In particular, the target ABEP assumes values of 10^{-5}, 10^{-6} and 10^{-7}. When $q = 1$, we have a conventional system. As a consequence, notice that the system cannot guarantee the target ABEP in much of the cell area. On the other hand, when q is reduced (OpT), the coverage is increased. For example, for $q = 2/3$ and $P_{b,t} = 10^{-5}$ the system ensures coverage in all the cell region. More specifically, with 1024-QAM in the region closest to the BS, 64-QAM in the intermediate region and with 4-QAM in the outermost cell region. However, when $P_{b,t}$ is reduced to 10^{-6} or 10^{-7}, the system cannot guarantee coverage in the outermost cell region, but it should be noted that OpT guarantees these low ABEPs in a large cell area considering that channel coding is not used and that information is not transmitted only one third of the time. When q is reduced to $1/2$ or to $1/3$, the modulation order with which the target ABEP is guaranteed increases in certain cell regions. For example, for $q = 1/3$ and $P_{b,t} = 10^{-5}$, a large cell region is covered by 1024-QAM. This could be interpreted as higher mean SE, but it is important to remember that, in this scenario, the system does not transmit two-thirds of the time. Therefore it is important to establish the mean SE values for each scenario.

Fig. 10 shows the mean SE as a function of the transmission probability, q, and the target ABEP, $P_{b,t}$ calculated with the coverage radii of Fig. 9. Observe that the lowest SE is obtained for a conventional system ($q = 1$). This occurs because the system cannot guarantee $P_{b,t}$ in a large cell region. On the other hand, the highest mean SE is obtained with $q = 2/3$ for all the target ABEPs despite the fact that coverage in the entire cellular region is not guaranteed when $P_{b,t} = 10^{-6}$ or $P_{b,t} = 10^{-7}$. However, because in this scenario the information is not transmitted only one third of

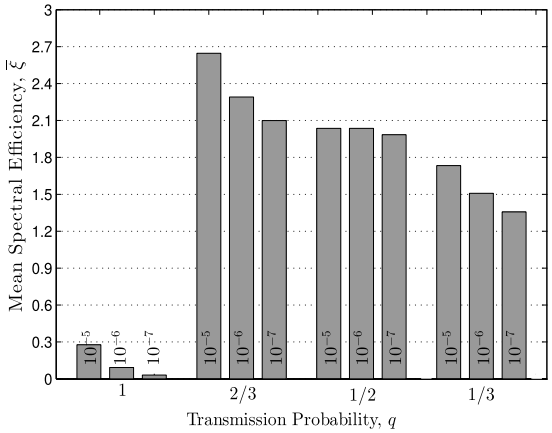

FIGURE 10. Mean spectral efficiency for the scenarios of Fig. 9.

[6]Category A terrain in the SUI path-loss model. The parameters associated to this scenario are detailed in Section V.

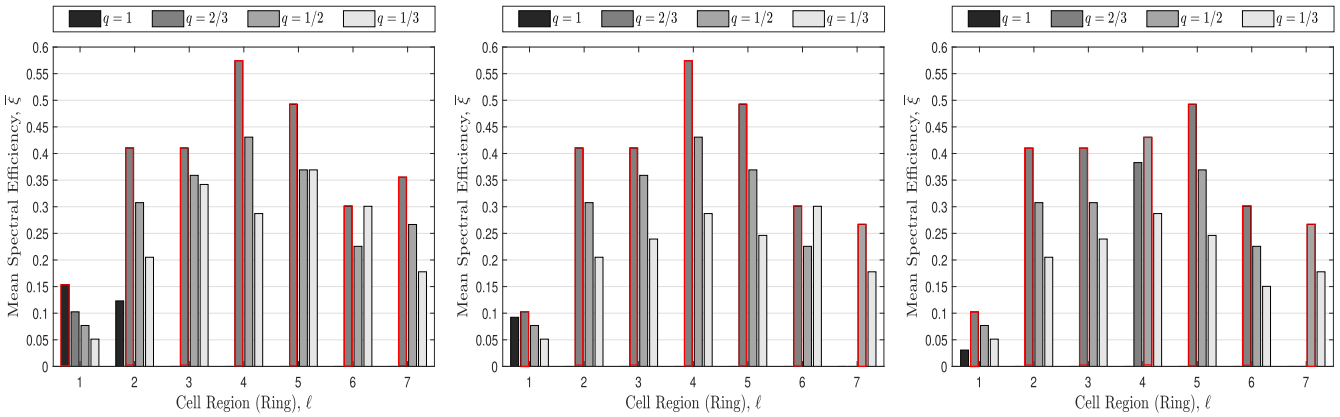

(a) $P_{b,t} = 10^{-5}$. (b) $P_{b,t} = 10^{-6}$. (c) $P_{b,t} = 10^{-7}$.

FIGURE 11. Mean spectral efficiency as a function of the cell region and parameterized by the transmission probability, q, and the target ABEP, $P_{b,t}$.

TABLE 2. Rician parameters as a function of the distance between UE and BS.

Ring	$\wp_{\ell-1} \leq r < \wp_\ell$	K_ℓ	Ω_ℓ
$\ell = 1$	100 m $\leq r <$ 200 m	$K_1 = 4$	$\Omega_1 = 5$
$\ell = 2$	200 m $\leq r <$ 400 m	$K_2 = 2$	$\Omega_2 = 3$
$\ell = 3$	400 m $\leq r <$ 600 m	$K_3 = 1$	$\Omega_3 = 2$
$\ell = 4$	600 m $\leq r <$ 800 m	$K_4 = 0.75$	$\Omega_4 = 1.75$
$\ell = 5$	800 m $\leq r <$ 1000 m	$K_5 = 0.5$	$\Omega_5 = 1.5$
$\ell = 6$	1000 m $\leq r <$ 1200 m	$K_6 = 0.25$	$\Omega_6 = 1.25$
$\ell = 7$	1200 m $\leq r <$ 1400 m	$K_7 = 0$	$\Omega_7 = 1$

TABLE 3. Mean SE for each cell region as a function of the transmission probability, q.

Ring	$\wp_{\ell-1} \leq r < \wp_\ell$	Transmission probability, q			
		1	2/3	1/2	1/3
$\ell = 1$	100 m $\leq r <$ 200 m	0.0308	0.1026	0.0769	0.0513
$\ell = 2$	200 m $\leq r <$ 400 m	0	0.4103	0.3077	0.2051
$\ell = 3$	400 m $\leq r <$ 600 m	0	0.4103	0.3077	0.2393
$\ell = 4$	600 m $\leq r <$ 800 m	0	0.3829	0.4308	0.2872
$\ell = 5$	800 m $\leq r <$ 1000 m	0	0.4923	0.3692	0.2462
$\ell = 6$	1000 m $\leq r <$ 1200 m	0	0.3009	0.2256	0.1504
$\ell = 7$	1200 m $\leq r <$ 1400 m	0	0	0.2667	0.1778

the time, $\bar{\xi}$ is maximized. At this point, it is important to remember that the mean SE is proportional to q (refer to (43)). As a consequence, the cell area can be reduced,[7] or, a lower transmission probability can be used at the cell edge. We also observe that as q is reduced to 1/2 or 1/3, the SE decreases, but coverage is guaranteed throughout the cell.

Finally, Fig. 11 shows the mean SE obtained for each cell region (each ring of Table 2) and parameterized by q, and the target ABEP, $P_{b,t}$. In the figure, the highest spectral efficiency for each cell region has been highlighted with red color. As an example, Table 3 shows the mean SE values for Fig. 11c. Based on these results, we determine that if $q = 1/2$ is used in the cell regions (rings) $\ell = 4$ and 7, and $q = 2/3$ in the rest of the cell, then coverage is guaranteed throughout the cell and the mean SE increases to 2.4139. This value is greater than any of those shown in Fig. 10 for $P_{b,t} = 10^{-7}$. A similar analysis can be performed for $P_{b,t} = 10^{-5}$ based on the results of Fig. 11a. In this case, the mean SE is maximized to 2.6974 when conventional transmission is used in the innermost cell region and OpT with $q = 2/3$ is used in the rest of the cell. For $P_{b,t} = 10^{-6}$, from Fig. 11b, the mean SE is maximized to 2.5573 if $q = 2/3$ it is used throughout the cell region. By the above, there is a direct relationship between the transmission probability, the SE and the coverage area. Thus, they must be jointly analyzed based on the requirements and the design of the opportunistic wireless system. In order to obtain the above results, certain S-QAM/NS-QAM schemes were chosen arbitrarily. However, in practice, modulation schemes must be selected based on transmission rate requirements or based on channel conditions [21]. Thus, another set of S-QAM/NS-QAM schemes can be used in order to maximize the system spectral efficiency depending on the operating conditions.

[7]The reduction of the cell area must be analyzed considering the complete design of the cellular network, once the cell size reduction implies a greater amount of BSs and therefore, a higher implementation cost.

VII. CONCLUSION

In this paper, the performance of opportunistic wireless systems operating in Rician fading channels was analyzed. Exact and approximate expressions were derived to evaluate the ABEP considering S-QAM ans NS-QAM modulations. In addition, the analysis of these expressions in the high SNR regime and the numerical results show that ABEP curves decay exponentially when they are plotted as a function of the SNR. It means that fading effects are highly mitigated because of the OpT. Moreover, it was observed that as the Rician K factor increases, the ABEP is reduced by a factor $(K + 1)\exp(-K)$ in the high SNR region.

When the transmission probability is reduced, the threshold for the fading amplitude increases. This produces an ABEP reduction, but the SE is also reduced because non-transmission probability increases. Therefore, transmission probability must be selected based on system

requirements to maximize the SE. Thus, we also proposed an algorithm to determine the coverage radius that can be provided with a certain modulation so that an ABEP is guaranteed in all the cell area. In addition, an expression to calculate the mean SE was derived considering the radii obtained with the algorithm. In particular, it was considered that the parameters of the Rician fading channel can change in the cellular area, that is, the shorter the distance between the BS and the UE, the greater the Rician K factor. Results showed that conventional transmission cannot ensure coverage in all the cell region when low ABEP values are required. On the other hand, OpT ensures a much larger coverage cell area and guarantees very low ABEPs even with high order modulations such as 128-QAM and 1024-QAM. In addition, as the transmission probability decreases, the coverage with higher order modulations increases, but the mean SE decreases.

Moreover, since simulations are typically time consuming and do not show the interdependence between the operating system parameters, the derived expressions are interesting analytical tools for designing opportunistic wireless networks once they allow to determine the scenarios that maximize the system mean SE. In particular, it was observed that the ABEP, the transmission probability, and the coverage area must be jointly analyzed in order to maximize the SE.

Aspects such as imperfect CSI or errors in the feedback link were not considered in this paper. Hence, they are interesting extensions for future research. Besides, generalized fading channels and the effects of channel dispersion can be also considered to analyze the performance of OpT. Finally, the use of OpT in new technologies such as massive multiple-input-multiple-output (mMIMO) is an option for future work.

REFERENCES

[1] *New Services and Applications with 5G Ultra-Reliable Low Latency Communications*, 5G Americas, Bellevue, WA, USA, Nov. 2018.

[2] A. Ghosh, A. Maeder, M. Baker, and D. Chandramouli, "5G evolution: A view on 5G cellular technology beyond 3GPP release 15," *IEEE Access*, vol. 7, pp. 127639–127651, Sep. 2019, doi: 10.1109/ACCESS.2019.2939938.

[3] A. Abdi, C. Tepedelenlioglu, M. Kaveh, and G. Giannakis, "On the estimation of the k parameter for the Rice fading distribution," *IEEE Commun. Lett.*, vol. 5, no. 3, pp. 92–94, Mar. 2001, doi: 10.1109/4234.913150.

[4] J. Proakis and M. Salehi, *Digital Communications*, 5th ed. New York, NY, USA: McGraw-Hill, 2008.

[5] C. I. Frison, H. C. Mora, and C. de Almeida, "Optimum rotation parameters for single and multiuser signal space diversity employing spatial diversity," *AEU, Int. J. Electron. Commun.*, vol. 107, pp. 275–281, Jul. 2019, doi: 10.1016/j.aeue.2019.05.032.

[6] M. Bilim, "A performance study on diversity receivers over κ-μ shadowed fading channels," *AEU, Int. J. Electron. Commun.*, vol. 112, Dec. 2019, Art. no. 152934, doi: 10.1016/j.aeue.2019.152934.

[7] N. O. Garzon, H. C. Mora, and C. de Almeida, "Performance evaluation of encoded opportunistic transmission schemes," *IEEE Access*, vol. 7, pp. 89316–89329, Jul. 2019, doi: 10.1109/ACCESS.2019.2927178.

[8] Q. Zhao and L. Tong, "Distributed opportunistic transmission for wireless sensor networks," in *Proc. IEEE Int. Conf. Acoust., Speech, Signal Process.*, May 2004, pp. III–833, doi: 10.1109/ICASSP.2004.1326674.

[9] N. V. O. Garzon, H. R. C. Mora, and C. de Almeida, "A hybrid transmission scheme employing opportunistic transmission and multiuser diversity," in *Proc. IEEE 13th Int. Conf. Wireless Mobile Comput., Netw. Commun. (WiMob)*, Oct. 2017, pp. 98–103, doi: 10.1109/WiMOB.2017.8115786.

[10] G. N. Orozco and C. de Almeida, "Performance evaluation of opportunistic wireless transmission in Rayleigh fading channels with co-channel interference," in *Proc. IEEE Latin-America Conf. Commun.*, Nov. 2013, pp. 1–6, doi: 10.1109/LatinCom.2013.6759826.

[11] N. O. Garzon, H. C. Mora, and C. de Almeida, "An opportunistic system to counteract fading and Gaussian interference effects under different modulation schemes," *IEEE Latin Amer. Trans.*, vol. 16, no. 11, pp. 2716–2721, Nov. 2018, doi: 10.1109/TLA.2018.8795112.

[12] S. Haykin, "Cognitive radio: Brain-empowered wireless communications," *IEEE J. Sel. Areas Commun.*, vol. 23, no. 2, pp. 201–220, Feb. 2005, doi: 10.1109/JSAC.2004.839380.

[13] P. S. Chauhan, S. Kumar, and S. K. Soni, "On the physical layer security over Beaulieu–Xie fading channel," *AEU, Int. J. Electron. Commun.*, vol. 113, Jan. 2020, Art. no. 152940, doi: 10.1016/j.aeue.2019.152940.

[14] J.-H. Lee, H.-M. Kim, and W. Choi, "Achievable ergodic secrecy rate in bursty interference channels with opportunistic user scheduling," *IEEE Trans. Commun.*, vol. 67, no. 11, pp. 7686–7699, Nov. 2019, doi: 10.1109/TCOMM.2019.2935196.

[15] N. V. O. Garzon, H. R. C. Mora, and C. de Almeida, "Performance analysis of opportunistic systems employing maximal ratio combining and antenna array," in *Proc. IEEE 84th Veh. Technol. Conf. (VTC-Fall)*, Sep. 2016, pp. 1–5, doi: 10.1109/VTCFall.2016.7881154.

[16] H. Nam, K. S. Ko, I. Bang, and B. C. Jung, "Achievable rate analysis of opportunistic transmission in bursty interference networks," *IEEE Commun. Lett.*, vol. 22, no. 3, pp. 654–657, Mar. 2018, doi: 10.1109/LCOMM.2017.2787983.

[17] L. Yang, H. Jiang, Q. Ye, Z. Ding, F. Fang, J. Shi, J. Chen, and X. Xue, "Opportunistic adaptive non-orthogonal multiple access in multiuser wireless systems: Probabilistic user scheduling and performance analysis," *IEEE Trans. Wireless Commun.*, vol. 19, no. 9, pp. 6065–6082, Sep. 2020, doi: 10.1109/TWC.2020.2999814.

[18] P. K. Jha, S. S. Shree, and D. S. Kumar, "An opportunistic-non orthogonal multiple access based cooperative relaying system over Rician fading channels," in *Proc. 4th Int. Conf. Recent Adv. Inf. Technol. (RAIT)*, Mar. 2018, pp. 1–5, doi: 10.1109/RAIT.2018.8388973.

[19] C. Yuzhi and Z. Baoyu, "An opportunistic cooperative transmission scheme and its BER performance in cognitive networks," in *Proc. IEEE 12th Int. Conf. Commun. Technol.*, Nov. 2010, pp. 987–990, doi: 10.1109/ICCT.2010.5688788.

[20] F. T. Hidalgo, N. O. Garzon, H. C. Mora, and J. Freire, "On the bit error rate of opportunistic wireless systems that employ non-square quadrature amplitude modulations," in *Proc. IEEE 4th Ecuador Tech. Chapters Meeting (ETCM)*, Nov. 2019, pp. 1–5, doi: 10.1109/ETCM48019.2019.9014876.

[21] P. K. Singya, P. Shaik, N. Kumar, V. Bhatia, and M.-S. Alouini, "A survey on design and performance of higher-order QAM constellations," Apr. 2020, *arXiv:2004.14708*. [Online]. Available: http://arxiv.org/abs/2004.14708

[22] J. Barry, E. Lee, and D. Messerschmitt, *Digital Communication*, 3th ed. New York, NY, USA: Springer, 2004.

[23] B. Mouhouche, D. Ansorregui, and A. Mourad, "High order non-uniform constellations for broadcasting UHDTV," in *Proc. IEEE Wireless Commun. Netw. Conf. (WCNC)*, Apr. 2014, pp. 600–605, doi: 10.1109/WCNC.2014.6952116.

[24] M. Fuentes, L. Christodoulou, and B. Mouhouche, "Non-uniform constellations for broadcast and multicast in 5G new radio," in *Proc. IEEE Int. Symp. Broadband Multimedia Syst. Broadcast. (BMSB)*, Jun. 2018, pp. 1–5, doi: 10.1109/BMSB.2018.8436805.

[25] A. Papoulis, *Probability, Random Variables, and Stochastic Processes*, 4th ed. New York, NY, USA: McGraw-Hill, 2002.

[26] M. Abramowitz and I. A. Stegun, *Handbook of Mathematical Functions With Formulas, Graphs and Mathematical Tables*. Washington, DC, USA: Department of Commerce, 1964.

[27] W. Lindsey, "Error probabilities for Rician fading multichannel reception of binary and N-ary Signals," *IEEE Trans. Inf. Theory*, vol. IT-10, no. 4, pp. 339–350, Oct. 1964, doi: 10.1109/TIT.1964.1053703.

[28] K. Cho and D. Yoon, "On the general BER expression of one- and two-dimensional amplitude modulations," *IEEE Trans. Commun.*, vol. 50, no. 7, pp. 1074–1080, Jul. 2002, doi: 10.1109/TCOMM.2002.800818.

[29] I. Gradshteyn and I. Ryzhik, *Table of Integrals, Series, and Products*, 7th ed. London, U.K.: Elsevier, 2007.

[30] H. C. Mora, N. O. Garzón, and C. de Almeida, "On the cellular spectral efficiency of MC-CDMA systems with MMSE multiuser detector employing fractional and soft frequency reuse," *AEU, Int. J. Electron. Commun.*, vol. 84, pp. 34–45, Feb. 2018, doi: 10.1016/j.aeue.2017.11.011.
[31] P. D. Katev, "Propagation models for WiMAX at 3.5 GHz," in *Proc. IEEE Elektro Conf.*, May 2012, pp. 61–65, doi: 10.1109/ELEKTRO.2012.6225572.
[32] *5G Spectrum—Public Policy Position*, GSMA, London, U.K., Nov. 2016.
[33] M. López-Benítez, "Outage probability and average error performance of modulation schemes under Nakagami-*q* (Hoyt) and Nakagami-n (Rice) fading channels," in *Proc. 10th Int. Symp. Commun. Syst., Netw. Digit. Signal Process. (CSNDSP)*, Prague, Czech Republic, Jul. 2016, pp. 1–6, doi: 10.1109/CSNDSP.2016.7573981.
[34] H. Carvajal, N. Orozco, D. Altamirano, and C. De Almeida, "Performance analysis of non-ideal sectorized SFR cellular systems in Rician fading channels with unbalanced diversity," *IEEE Access*, vol. 8, pp. 133654–133672, Jul. 2020, doi: 10.1109/ACCESS.2020.3010889.
[35] *User Equipment (UE) Radio Transmission and Reception*, document TS 38.101-2, 3GPP, Version 15.3.0, Oct. 2018.
[36] *Physical Channels and Modulation*, document TS 38.211, 3GPP, Version 15.3.0, Oct. 2018.
[37] J. Proakis, "Probabilities of error for adaptive reception of M-phase signals," *IEEE Trans. Commun.*, vol. COM-16, no. 1, pp. 71–81, Feb. 1968.

NATHALY OROZCO GARZÓN received the electronic and telecommunications engineering degree from Armed Forces University–ESPE, Sangolqui, Ecuador, in 2011, and the M.Sc. and Ph.D. degrees in electrical engineering from the University of Campinas (UNICAMP), Brazil, in 2014 and 2018, respectively. She is currently a Full Professor with the Universidad de Las Américas (UDLA), Quito, Ecuador. Her research interests include digital communications with specific emphasis on orthogonal and non-orthogonal multiple access, fading channels, MIMO, cognitive systems, opportunistic transmissions, and 5G technologies.

HENRY CARVAJAL MORA (Member, IEEE) received the B.Sc. degree (Hons.) in electronics and telecommunications engineering from Armed Forces University–ESPE, Ecuador, in 2009, and the M.Sc. and Ph.D. degrees in electrical engineering from the School of Electrical and Computer Engineering (FEEC), University of Campinas (UNICAMP), Brazil, in 2014 and 2018, respectively. He was the Director of the Technology Transfer Area with the Education, Science and Technology Secretariat (SENESCYT), Ecuador, in 2018. He is currently a Full Professor with the Universidad de Las Américas (UDLA), Quito, Ecuador. His research interests include fading channels, diversity-combining systems, orthogonal and non-orthogonal multiple access, multiuser detection, MIMO, 5G, and B5G technologies.

FERNANDO ALMEIDA GARCÍA received the B.Sc. degree in electrical and telecommunications engineering from Armed Forces University–ESPE, Sangolqui, Ecuador, in 2012, and the M.Sc. degree in electrical engineering from the University of Campinas (UNICAMP), Brazil, in 2015, where he is currently pursuing the Ph.D. degree. Since 2014, he has been working with Bradar Indústria S.A., a branch of Embraer Defense and Security, in the design and development of novel radar signal processing techniques. His research interests include radar systems and wireless communications.

CARLOS DANIEL ALTAMIRANO (Member, IEEE) received the electronic and telecommunications engineering degree from the Universidad de las Fuerzas Armadas–ESPE, Sangolqui, Ecuador, in 2008, and the M.Sc. degree in electrical engineering from the University of Campinas (UNICAMP), Brazil, in 2011, where he is currently pursuing the Ph.D. degree. He is currently a Full Professor with the Universidad de las Fuerzas Armadas-ESPE. His research interests include digital communications with specific emphasis on multiple access techniques, fading channels, MIMO, error control coding, software defined radio, and 5G technologies.